Synthesis and biological evaluation of radio-iodinated benzimidazoles as SPECT imaging agents for NR2B subtype of NMDA receptor

Takeshi Fuchigami [a,c], Hiroshi Yamaguchi [b], Mikako Ogawa [a], Le Biao [a], Morio Nakayama [c], Mamoru Haratake [c], Yasuhiro Magata [a,b,*]

[a] Photon Medical Research Center, Hamamatsu University School of Medicine, Hamamatsu 431-3192, Japan
[b] Molecular Imaging Frontier Research Center, Hamamatsu University School of Medicine, Hamamatsu 431-3192, Japan
[c] Graduate School of Biomedical Sciences, Nagasaki University, 1-14 Bunkyo-machi, Nagasaki 852-8521, Japan

ABSTRACT

In this study, the benzimidazole derivatives were synthesized and evaluated as imaging agents for the NR2B subtype of NMDA receptor. Among these ligands, 2-{[4-(4-iodobenzyl)piperidin-1-yl]methyl}benzimidazol-5-ol (8) and N-{2-[4-(4-iodobenzyl)-piperidin-1-ylmethyl]benzoimidazol-5-yl}-methanesulfonamide (9) exhibited high affinity for the NR2B subunit (K_i values; 7.28 nM for 8 and 5.75 nM for 9). In vitro autoradiography experiments demonstrated high accumulation in the forebrain regions but low in the cerebellum for both [125I]8 and [125I]9. These regional distributions of the radioligands correlated with the expression of the NR2B subunit. The in vitro binding of these ligands was inhibited by NR2B antagonist but not by other site ligands, which suggested the high selectivity of [125I]8 and [125I]9 for the NR2B subunit. In mice, the regional brain uptakes of [125I]8 and [125I]9 at 5–180 min after administration were 0.42–0.56% and 0.44–0.67% dose/g, respectively. The brain-to-blood ratio of [125I]8 at 180 min was reduced by 34% in the presence of non-radioactive ligands and by 59% in the presence of the NR2B ligand Ro-25,6981. These results indicated that [125I]8 could be partially bound to the NR2B subunit in vivo. Although the brain uptake of these benzimidazole derivatives was too low to allow for in vivo SPECT imaging, these compounds might be useful scaffolds for the development of imaging probes specific for the NMDA receptors.

© 2010 Elsevier Ltd. All rights reserved.

1. Introduction

The N-methyl-D-aspartate (NMDA) receptor, a member of the glutamate receptors, plays an important role in the neurotransmission function of the central nervous system (CNS).[1] Overactivation of the NMDA receptor, however, is thought to cause various disorders, such as ischemia, stroke, Parkinson's Disease, Alzheimer's Disease, Huntington's Disease, and schizophrenia.[2–6] NMDA receptors are heteromers, which contain an NR1 subunit and one or more types of the different NR2 subunits (NR2A-D).[7] NR1 subunit has only one gene (eight splice variants) with ubiquitous distribution in the brain. NR2 subunits, on the other hand, exhibit distinct distribution in the brain, which determine the synaptic localization and function of the NMDA receptor. The NR2A subunit is widely distributed throughout the brain; but, the NR2B subunit is confined in the forebrain region, including the cerebral cortex, hippocampus, and olfactory bulb. The NR2C and NR2D are localized in the cerebellum and diencephalus/lower brain stem, respectively. The NR2A and NR2B are known to be the predominant NR2

subunits in the adult forebrain.[8] It is suggested that NR2A-containing NMDA receptors are involved in prosurvival signaling; thereby, they exert a neuroprotective action against glutamate receptor-dependent apoptotic neuronal injuries.[9–11] On the other hand, an increasing number of reports have demonstrated the importance of the NR2B subunit in determining the pharmacological and functional properties of the NMDA receptor. The NR2B has been implicated in modulating functions, such as learning, memory processing, and feeding behaviors, as well as being involved in a number of human disorders.[12] It is suggested that activation of the NR2B-containing NMDA receptor initiates apoptotic signaling cascades and promotes neuronal death.[9–11] Recent progress in molecular biology revealed the in vitro function of the NR2B-containing NMDA receptor considerably. However, its function in the living brain is not well understood due to the lack of visualizing method in vivo. Positron emission tomography (PET) and single photon emission computed tomography (SPECT) are the most efficient imaging methods for in vivo measurement of neurotransmitter receptors and enzymes in the brain. Our study, as well as other studies, has developed several radioligands for the NR2B subunit of the NMDA receptor (Fig. 1). These ligands showed similar accumulation pattern with the localization of expression of the NR2B

* Corresponding author. Tel./fax: +81 53 435 2398.
  E-mail address: magata@hama-med.ac.jp (Y. Magata).
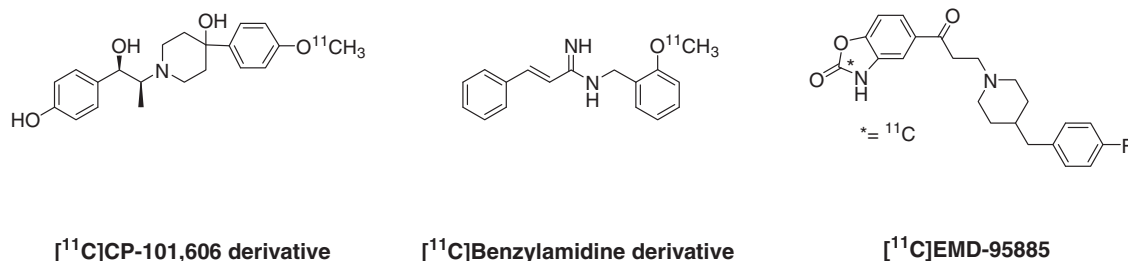
Figure 1. Structure of radioligands for imaging of the NR2B subtype of the NMDA receptor.

subunit only under in vitro condition but not in vivo.[13–19] Among these ligands, only [^{11}C]EMD-95885 showed significant reduction of the in vivo brain uptake by treatment with the NR2B ligand.[16] Although the inhibition pattern was inconsistent with NR2B expression, this chemical structure might be a useful lead for the development of potential imaging probes. Recently, a new series of benzimidazole derivatives **1** and **2** are developed as novel NR2B antagonists (Fig. 2),[20] which have similar chemical structures with EMD-95885. For example, compound **1a** showed excellent affinity for the NR2B subunit (K_i = 1.5 nM). Introduction of a hydrophobic substituent into the R_2-position of benzimidazoles, such as compound **1**, maintained receptor affinity.[20–22] On the bases, we designed new SPECT imaging agents, which introduced ^{125}I atom into the R_2-position of benzimidazoles. In this study, [^{125}I] labeled benzimidazole derivatives were synthesized and the in vitro binding properties and in vivo brain uptake characteristics in rodents were examined. It is reported that ^{11}C labeled 4-acetoxy derivative of L-703,717, which is a PET ligand for glycine site of NMDA receptor, can be a substrate of P-gp.[23] However it is not clear if the NR2B ligands are substrates of P-gp. Some of NR2B ligands such as ifenprodil and benzidazoles in this series have acidic phenol group. It has been shown that organic anion transporter is responsible for the elimination of several acidic drugs from the brain across the BBB.[24] Therefore the effect of P-gp and OAT on the in vivo uptake of [^{125}I]benzimidazoles were also investigated.

2. Results and discussion

2.1. Chemistry

Based on the previous structure–activity relationship studies,[20–22] the SPECT imaging agent candidates **8**, **9**, and **13** were designed, in which an iodine atom was introduced into the 4′-position (R_2-position) of benzyl- or phenoxy-piperidine group of benzimidazoles. Lead compound **1a** was synthesized according to the literature.[20] The 4′-iodo substituted benzylpiperidine derivatives (**8** and **9**) were

synthesized as shown in Scheme 1. Alkylation of compound **3**[25] with ethyl bromoacetate gave **4** (71% yield), followed by a bromo-to-tributyltin exchange reaction gave tributyltin derivative **5** for yields of 53%. Compound **5** was allowed to react with iodine in CCl$_4$ to give the iodo derivative **6** (68% yield). Compound **6** was hydrolyzed, followed by general amide coupling reaction with the corresponding phenylenediamines. Dehydration of the amidated products in acetic acid at reflux gave the benzimidazoles **7** and **9** for yields of 55% and 53%, respectively. Compound **7** was converted to **8** by desmethylation with HBr (63% yield). The target iodo phenoxypiperidine derivative (**13**) was synthesized as shown in Scheme 2. Phenoxypiperidine **11** was synthesized according to the method of Scheme 1 starting from compound **10**[26] for yield of 45%. Benzimidazole **12** was obtained by the same procedure for the synthesis of compound **7** for yield of 73%. Finally, compound **12** was desmethylated by BBr$_3$ to give **13** (77% yield).

2.2. In vitro binding assays

The binding affinities (K_i values) of benzimidazole derivatives for the NR2B subunit of NMDA receptor were evaluated with displacement studies of the typical NR2B antagonist, [^{3}H]ifenprodil, to rat cortical synaptic membranes according to the literature.[27] Trifluoroperazine was used to block the binding of [^{3}H]ifenprodil in rat brain membranes to sites other than the NMDA receptors. As shown in Table 1, lead compound **1a** showed excellent affinity (K_i = 3.09 nM) for the NR2B subunit, which was consistent with the results by using hNR1a/NR2B receptors expressed in Ltk-cells (K_i = 1.50 nM) reported in the literature.[20] Introduction of an iodine atom in R_2 resulted in a slight reduction of binding affinity; however, high affinity for the NR2B subunit (K_i values; 7.28 and 5.75 nM for **8** and **9**, respectively) was maintained. On the other hand, phenoxypiperidine benzimidazole **13** exhibited a 4.5-fold lower affinity (K_i = 32.5 nM) than compound **8**. These results suggested that the presence of phenoxypiperidine frame, instead of the benzylpiperidine, negatively influenced the in vitro binding affinity for this class of compound. In the recent report, the indole-carboxamide derivatives, with an oxygen atom substituted in the X-position, have several-fold lower affinity than the compounds with methylene group. On the contrary, comparable affinities were shown between benzimidazole-carboxamide derivatives substituted with methylene group and oxygen atom in X-position.[22] Therefore, it might be difficult to fit the binding space for phenoxypiperidine derivatives in the NR2B antagonist binding site. Since **8** and **9** had high affinity for the NR2B subunit of the NMDA receptor, these ligands were selected to carry out further biological evaluations on the corresponding I-125-labeled probes.

2.3. Radiochemistry

Trimethyltin precursors **14** and **15** were synthesized from **8** and **9**, respectively, by an iodo-to-trimethyltin exchange reaction (53% yield for **14** and 97% yield for **15**). To obtain [^{125}I]**8** and [^{125}I]**9**, the

1

1a; R$_1$= OH, R$_2$= H

2

R$_1$= OH, NHSO$_2$Me
R$_2$= Me, F, Cl
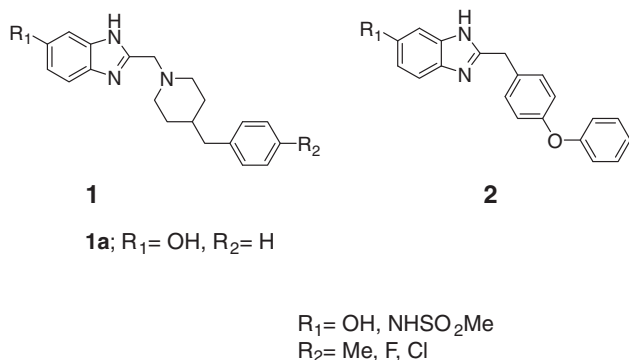
Figure 2. Structure of benzimidazoles as NR2B antagonists.
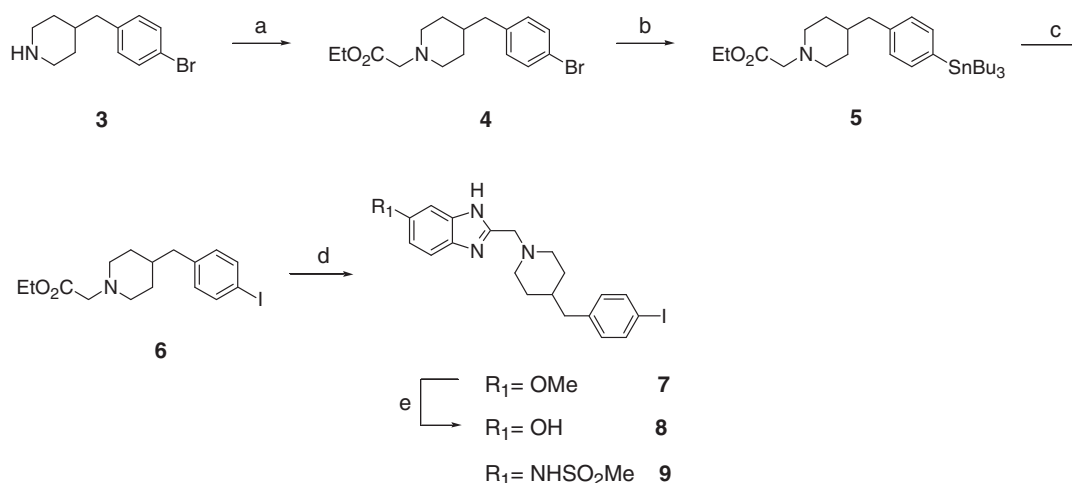
Scheme 1. Preparation of benzylpiperidine derivatives (**8** and **9**). Reagent and conditions: (a) ethyl bromoacetate, diisopropylethylamine, DMF, rt, 71%; (b) (Bu₃Sn)₂, (Ph₃P)₄Pd, toluene, 110 °C, 53%; (c) I₂, CCl₄, rt, 68%; (d) (1) HCl, 100 °C, (2) EDC, HOAt, triethylamine, 4-substituted phenylenediamine, DMF, rt, (3) acetic acid, 140 °C, 55% for **7**, 53% for **9**; (e) HBr/H₂O, 100 °C, 63%.
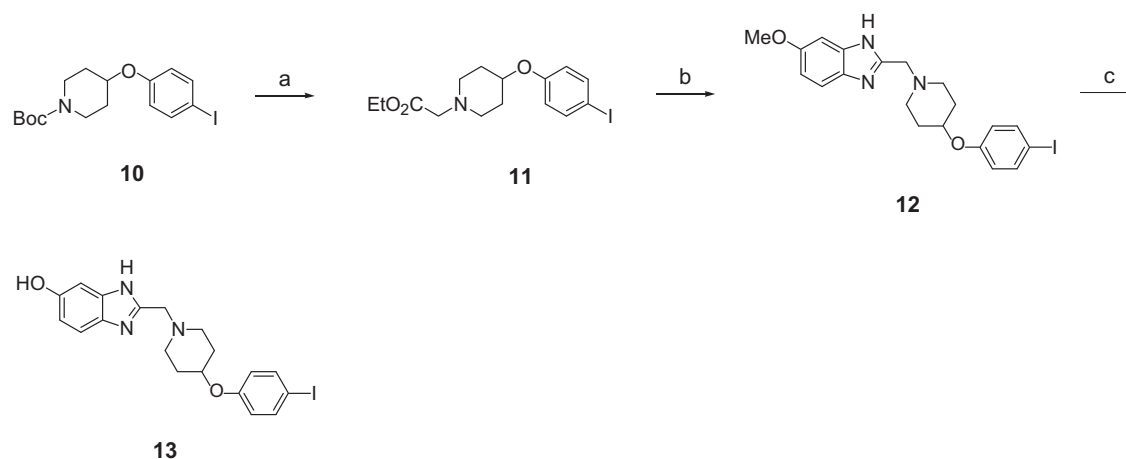
Scheme 2. Preparation of phenoxypiperidine derivative (**13**). Reagent and conditions: (a) (1) TFA, CH₂Cl₂, rt, (2) ethyl bromoacetate, diisopropylethylamine, DMF, rt, 45%; (b) (1) HCl, 100 °C, (2) EDC, HOAt, triethylamine, 4-substituted phenylenediamine, DMF, rt, (3) acetic acid, 140 °C, 73%; (c) BBr₃, CH₂Cl₂, rt, 77%.

Table 1
In vitro binding affinity (K_i) of new benzimidazole derivatives for the NR2B subtype of the NMDA receptor and octanol/phosphate buffer distribution co-efficient (log D)

Compounds	R_1	R_2	X	K_i^a (nM)	K_i^b (nM)	log $D_{7.4}^c$
Ifenprodil					20.0 ± 4.89	
1a	OH	H		1.50	3.09 ± 0.22	
8	OH	I	CH₂		7.28 ± 2.93	3.95
9	NHSO₂Me	I	CH₂		5.75 ± 1.19	3.54
13	OH	I	O		32.5 ± 16.3	3.74

[a] Data from Ref. 20. The assay was inhibition study of ³H-[(E)-N1-(2-methoxy-benzyl)cinnamamidine] binding to hNR1a/NR2B receptors expressed in Ltk-cells.

[b] The K_i values were obtained by the method in Ref. 25. Each value (mean ± SD) was determined triplicate using rat cortical membrane homogenates in HEPES-KOH buffer.

[c] The partition co-efficient between n-octanol and sodium phosphate buffer at pH 7.4 (log $D_{7.4}$) was determined by conventional shake-flask method (n = 3).

corresponding trimethyltin precursors were allowed to react with [¹²⁵I]NaI (carrier-free) in the presence of H₂O₂ and HCl at room temperature for 40 min by a similar method in the literature[28] (Scheme 3). The resulting I-125 labeled crude products were purified by HPLC. The radiochemical yields based on [¹²⁵I] NaI were 85–90% and 78–81% for [¹²⁵I]**8** and [¹²⁵I]**9**, respectively.

2.4. In vitro autoradiography

In vitro regional distributions of [¹²⁵I]benzimidazoles on the rat brain sections were evaluated by a method mentioned in the literature.[13] As shown in the autoradiogram in Figure 3, both [¹²⁵I]**8** and [¹²⁵I]**9** showed high accumulation in the forebrain region (cerebral cortex and hippocampus), which is an NR2B-rich region, and lower uptake in the cerebellum, which is an NR2B-poor region (Fig. 3A and B). These distribution patterns were similar to [³H]CP-101,606,[29] as well as to the mRNA distribution of the NR2B sub-unit.[30] Non-specific binding was determined in the presence of corresponding non-radioactive benzimidazoles (10 μM), which resulted in a significant decrease in [¹²⁵I]**8** and [¹²⁵I]**9** accumulations in the forebrain region compared with total binding as visualized in Figure 3C and D and quantified in Figure 3E and F,
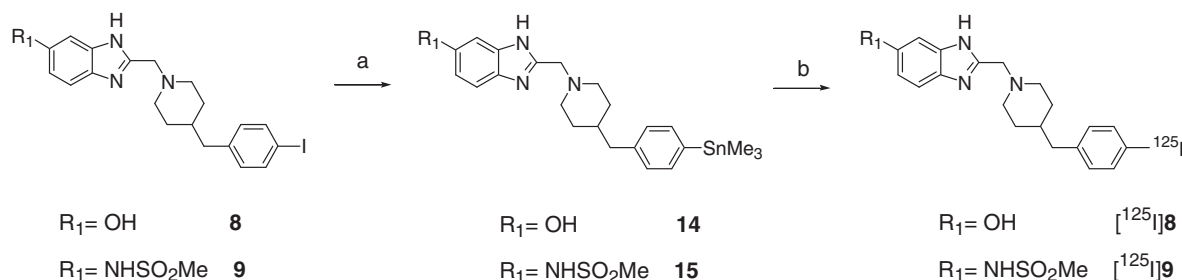
Scheme 3. Preparation of [^{125}I]8 and [^{125}I]9. Reagent and conditions: (a) (Me$_3$Sn)$_2$, (Ph$_3$P)$_4$Pd, toluene, 110 °C, 53% for **14** and 97% for **15**; (b) [^{125}I]NaI, H$_2$O$_2$, HCl, EtOH, rt, 85–90% for [^{125}I]**8** and 78–81% for [^{125}I]**9**.

respectively. Almost no specific binding of both ligands exists in the cerebellum. The specific binding of [^{125}I]**8** was higher than [^{125}I]**9** in the forebrain regions (Fig. 3E and F). These [^{125}I]benzimidazoles showed similar binding property with C-11-labeled analog of CP-101,606, which is a high-affinity radioligand for the NR2B subunit.[13] However, their specific bindings were lower than the [^{11}C]CP-101,606 analog. The high lipophilic property of [^{125}I]**8** and [^{125}I]**9** was attributed to. The log $D_{7.4}$ values of **8** and **9** were 3.95 and 3.54, respectively, as shown in Table 1, which are higher than the [^{11}C] CP-101,606 analog (log P = 0.75).

In order to investigate the specific binding of [^{125}I]**8** and [^{125}I]**9** to the NR2B subunit of the NMDA ion channel, in vitro inhibition studies on rat brain region using Ro-25,6981 (NR2B antagonist) were carried out. Since it is reported that several ifenprodil-like antagonists bind to α1-adrenergic and σ receptor,[31,32] the effects of prazosin (α$_1$-adrenergic receptor antagonist) and DTG (σ receptor antagonist) in blocking these receptors in the inhibition studies were examined. In result, the in vitro bindings of [^{125}I]**8** and [^{125}I]**9** in the cerebral cortex and hippocampus were inhibited only by the NR2B selective antagonist, Ro-25,6981, as shown in Table 2. On the contrary, no ligands inhibited the bindings in the cerebellum. These results indicated that [^{125}I]**8** and [^{125}I]**9** selectively bind to the NR2B subunit. Therefore, this study attempted to carry out in vivo studies to validate the effectiveness of these [^{125}I] benzimidazoles as SPECT imaging agents for the NR2B-subunit-containing NMDA receptor.

2.5. In vivo pharmacology

The biodistribution studies of [^{125}I]**8** and [^{125}I]**9** were performed by using normal mice and the results were shown in Table 3. Initial brain uptake of [^{125}I]**8** was 0.21% dose/g at 0.5 min after intravenous
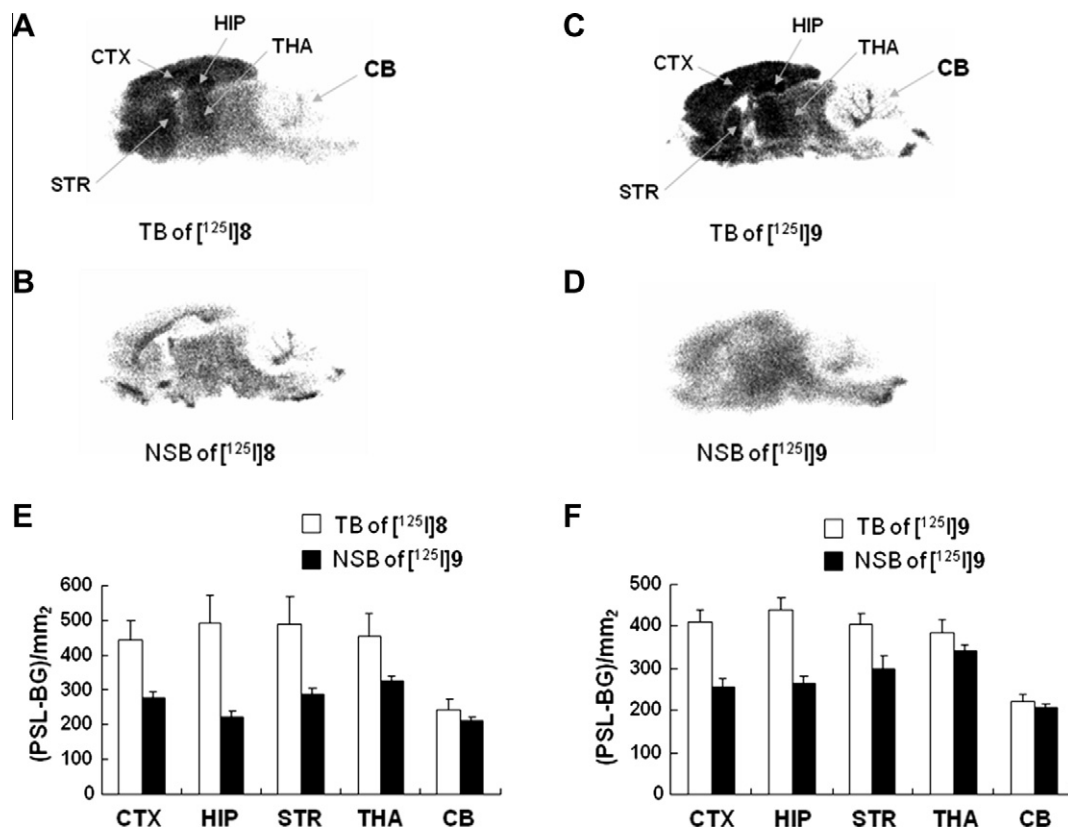
Figure 3. Autoradiogram of in vitro total binding (TB) of [^{125}I]8 (A), non-specific binding (NBS) of [^{125}I]8 (B), total binding of [^{125}I]9 (C), and non-specific binding of [^{125}I]9 (D) to rat brain sagittal sections. The quantified values of [^{125}I]8 (E) and [^{125}I]9 (F) in the cerebral cortex, hippocampus, and cerebellum were expressed as (PSL-BG)/mm$_2$ (mean ± SD, n = 4–6). Non-specific binding was determined in the presence of corresponding non-radioactive benzimidazoles (10 μM). *P <0.01 in comparison to the control group (Mann–Whitney U-test).

Table 2
Effects of drugs on in vitro binding of [^{125}I]benzimidazoles to rat brain slices

Ligands	% control binding[a]					
	[^{125}I]**8**			[^{125}I]**9**		
	Cerebral cortex	Hippocampus	Cerebellum	Cerebral cortex	Hippocampus	Cerebellum
Ro-25,6981	58.3	50.9	91.8	58.1	59.0	89.3
Prazosin	95.6	92.6	102.9	92.8	95.5	97.0
DTG	93.5	104.6	101.2	93.0	107.6	103.6

[a] Average values obtained by at least triplicate slices from three rats.

injection; whereas, the uptake of [^{125}I]**9** was 0.32% dose/g at the corresponding time. Both ligands showed very low brain-to-blood ratio (0.07) at 0.5 min. Radioactivity of [^{125}I]**8** and [^{125}I]**9** in the brain increased with time and peaked at 180 min after administration (0.56% and 0.67% dose/g, respectively). Accordingly, brain-to-blood ratio of these ligands rose to 1.99 and 1.23 at 180 min, respectively. High hepatic uptake of [^{125}I]**8** and [^{125}I]**9** was observed, which peaked to 32.22% and 17.81% dose/g at 180 min, respectively. The amount of radioactivity of these tracers in the kidney was also high (5.35–12.20% and 3.26–15.23% dose/g, respectively). The distribution patterns in peripheral tissues could be attributed to the high lipophilic property of these [^{125}I]benzimidazoles. These ligands showed almost homogenous brain distribution at 5–360 min after intravenous administration (Fig. 4), which was inconsistent with the localization of expression of the NR2B subunit. The results for [^{125}I]benzimidazoles were similar to other radioligands for the NR2B subunit.[13–16] Metabolisms of [^{125}I]**8** and [^{125}I]**9** in the mouse brain were analyzed by radio-TLC of brain homogenates obtained at 180 min post-injection; and 77% and 85%, respectively, of the parent compounds remained unchanged (data not shown). Thus, metabolism could have minimal effect the distribution pattern of [^{125}I]**8** and [^{125}I]**9**. The results of this study showed that in vitro specific binding and in vivo brain uptake to blood radioactivity ratio of [^{125}I]**8** were higher than [^{125}I]**9**. Therefore, in vivo experiments on [^{125}I]**8** were further performed.

The specificity of regional brain binding of [^{125}I]**8** for the NR2B subunit was studied by blocking studies using non-radioactive **8**

and Ro-25,6981 (3 mg/kg, intravenously), which were administered 30 min prior to injection of the radioligand. Since brain uptake of [^{125}I]**8** peaked at 180 min as shown in Table 3, regional brain distribution at 180 min after the radiotracer injection was determined. As shown in Figure 5, pre-injection of non-radioactive **8** resulted in a significantly increased blood radioactivity of [^{125}I]**8** ($P < 0.01$) compared with the control group. Altogether, the liver uptake was significantly decreased ($P < 0.01$). On the other hand, the brain uptake was increased slightly. Pre-administration of the NR2B selective antagonist, Ro-25,6981, had no effect on blood radioactivity of [^{125}I]**8**. The hepatic uptake of [^{125}I]**8** was slightly increased but the regional brain uptake was slightly decreased. It should be noted that both groups treated with cold **8** and Ro-25,6981 showed a markedly lower brain-to-blood ratio of [^{125}I]**8** than the control group (Fig. 5D). Considering these results, [^{125}I]**8** could have specific binding component in the NR2B subunit under in vivo condition, which was similar to [^{11}C]EMD-95885.[16] However, both [^{125}I]**8** and [^{11}C]EMD-95885 demonstrated reduced radioactivity in the NR2B poor region, cerebellum, even in the presence of NR2B ligands, which was unexplainable.

On the other hand, the brain uptake of commonly used PET radioligands, such as [^{11}C]raclopride and [^{11}C]DASB, was higher than [^{125}I]**8**.[33,34] Considering these facts, the brain permeability of [^{125}I]**8** could be inadequate for the visualization of NR2B subtype of the NMDA receptor by SPECT. All of the radioligands for NR2B subunit including benzidazoles in this report were inadequate BBB permeability. Log P (or log $D_{7.4}$) values of [^{125}I]**8**, [^{125}I]**9**, and

Table 3
Biodistribution data for ^{125}I labeled benzimidazoles in normal ddY mice[a]

Organ	0.5 min	5 min	30 min	60 min	180 min	360 min
[^{125}I]**8**						
Blood	3.22 ± 0.58	1.15 ± 0.06	0.67 ± 0.11	0.75 ± 0.13	0.30 ± 0.11	0.28 ± 0.11
Liver	14.68 ± 3.50	25.03 ± 4.20	28.99 ± 6.31	30.50 ± 6.60	32.22 ± 6.56	30.16 ± 1.83
Kidney	5.35 ± 0.91	12.20 ± 3.18	11.20 ± 2.65	10.34 ± 1.60	7.74 ± 1.32	5.46 ± 0.67
Intestine	4.02 ± 0.64	1.83 ± 0.33	2.39 ± 0.79	2.35 ± 0.47	4.55 ± 1.03	5.89 ± 1.05
Stomach	0.72 ± 0.16	1.93 ± 0.40	2.54 ± 0.81	2.16 ± 0.24	2.51 ± 0.55	2.17 ± 0.75
Spleen	0.50 ± 0.32	5.66 ± 1.25	5.91 ± 1.25	4.65 ± 0.51	4.25 ± 0.69	3.79 ± 0.43
Pancreas	0.49 ± 0.13	5.74 ± 2.45	6.10 ± 1.42	6.35 ± 1.25	6.53 ± 1.95	8.76 ± 0.37
Heart	1.47 ± 0.29	5.39 ± 0.33	2.31 ± 0.48	1.87 ± 0.41	1.58 ± 0.16	1.58 ± 0.11
Lung	6.60 ± 0.95	14.48 ± 2.52	8.16 ± 2.37	7.54 ± 2.19	4.75 ± 0.33	3.44 ± 0.80
Brain	0.21 ± 0.03	0.42 ± 0.06	0.44 ± 0.07	0.48 ± 0.09	0.56 ± 0.06	0.55 ± 0.14
Brain-to-blood ratio	0.07 ± 0.02	0.36 ± 0.03	0.67 ± 0.12	0.64 ± 0.06	1.99 ± 0.57	2.23 ± 0.99
[^{125}I]**9**						
Blood	4.74 ± 1.59	0.95 ± 0.40	0.53 ± 0.08	0.54 ± 0.08	0.55 ± 0.12	0.36 ± 0.10
Liver	4.60 ± 2.69	19.35 ± 9.22	16.67 ± 2.84	13.74 ± 1.72	17.81 ± 4.07	10.93 ± 2.51
Kidney	3.26 ± 1.64	10.99 ± 4.46	8.79 ± 0.91	8.52 ± 1.98	15.23 ± 2.31	10.51 ± 1.97
Intestine	0.55 ± 0.31	1.58 ± 0.75	3.07 ± 0.50	3.79 ± 0.69	7.82 ± 1.22	6.49 ± 1.77
Stomach	0.42 ± 0.22	1.28 ± 0.47	2.24 ± 0.46	2.40 ± 1.05	4.04 ± 0.83	3.56 ± 1.28
Spleen	0.90 ± 0.61	3.19 ± 1.43	2.91 ± 0.42	2.78 ± 0.57	2.85 ± 0.74	1.60 ± 0.26
Pancreas	0.92 ± 0.46	3.09 ± 1.59	3.71 ± 0.69	4.55 ± 1.14	5.39 ± 1.18	3.72 ± 0.59
Lung	9.07 ± 5.18	5.83 ± 1.29	4.29 ± 0.32	4.35 ± 0.38	6.93 ± 0.36	3.62 ± 0.21
Heart	3.82 ± 1.65	3.52 ± 2.19	1.86 ± 0.94	1.70 ± 0.73	1.61 ± 2.29	0.93 ± 0.55
Brain	0.32 ± 0.12	0.44 ± 0.19	0.50 ± 0.07	0.52 ± 0.07	0.67 ± 0.08	0.47 ± 0.09
Brain-to-blood ratio	0.07 ± 0.01	0.46 ± 0.09	0.94 ± 0.13	1.00 ± 0.26	1.23 ± 0.16	1.34 ± 0.28

[a] [^{125}I]Benzimidazoles (14.8 kBq) were injected intravenously via tail vein into ddY mice (male, 6 W, 30–35 g). Values were presented as mean ± SD (% dose/g, n = 5–6).

■ 5min □ 30min ▨ 60min ▤ 180min ▨ 360min
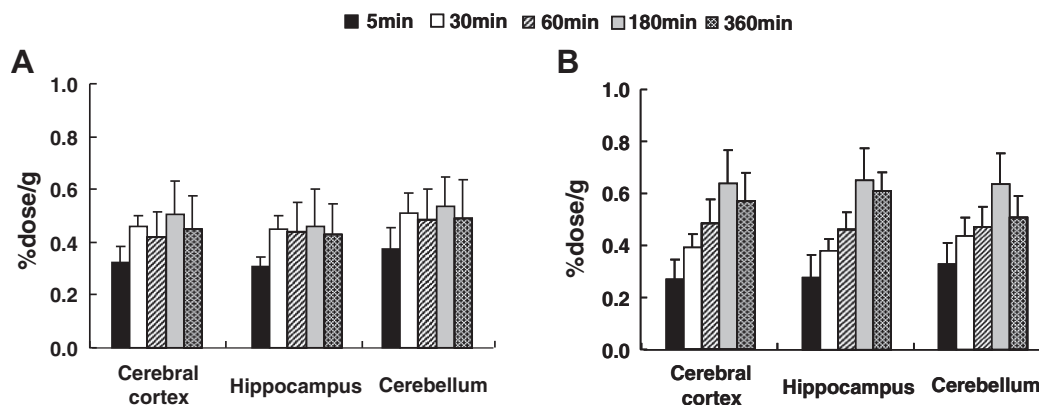
Figure 4. Regional brain uptake of [^{125}I]**8** (A) and [^{125}I]**9** (B) in normal ddY mice. [^{125}I]Benzimidazoles (148 kBq) were injected intravenously via mice tail vein.

^{11}C labeled CP-101,606 analog were 3.95, 3.54, and 0.75.[13] Log P values of 5-[3-(4-benzylpiperidin-1-yl)prop-1-ynyl]-1,3-dihydro-benzoimidazol-2-[11C]one[14] and [^{11}C]EMD-95885[16] were not reported, however, calculated by ChemDraw Ultra to be 3.36 and 3.40, respectively. These ligands are not within the optimal range (1.0–3.0) for compounds expected to penetrate the BBB.[35] Therefore log P value might be one of the reasons that the ligands showed low brain uptake. Another reason was thought to be high uptake of NR2B ligands in lung. The basic piperidine group in the ligands might cause these accumulation proclivities. Alternatively, lower molecular weight derivatives might be necessary to increase BBB permeability.

Another likely reason for the low uptake could be the excretion from brain tissue by the efflux systems of the BBB. It has been shown that many radioligands for mapping neuroreceptors are substrates for P-gp.[36–38] It is reported that several acidic drugs are eliminated by the OAT from the brain across the BBB.[24] Since the phenolic group in **8** has acidic moiety, there is a possibility that

the brain uptake of [^{125}I]**8** is effluxed by OAT. Therefore, the effect of P-gp and OAT to the in vivo brain uptake of [^{125}I]**8** was analyzed.

Pretreatment with CsA (Cyclosporine A) (substrate of P-gp, 50 mg/kg) or probenecid (substrate of OAT, 200 mg/kg) by intravenous injection on mice tail vein 30 min before [^{125}I]**8** administration was followed by examination of biodistribution 180 min later. As shown in Table 4, pretreatment with CsA resulted in the reduction of blood radioactivity level of [^{125}I]**8** but increase in the brain uptake in the CsA group compared with the control group. Therefore, the brain-to-blood ratio was 1.6-fold higher than the control group. Although P-gp is known to be present in the liver and kidney,[39] the effect of CsA to the uptake of [^{125}I]**8** in the liver and kidney is nil. In contrast, pretreatment with probenecid increased the brain uptake but decreased the blood radioactivity level of [^{125}I]**8**. The brain-to-blood ratio in the probenecid group was 1.3-fold higher than the control group. The uptake of [^{125}I]**8** in the kidney was significantly reduced relative to the control group. The hepatic uptake of [^{125}I]**8**, on the other hand, demon-

■ Control □ 8 ▨ Ro,25,6981
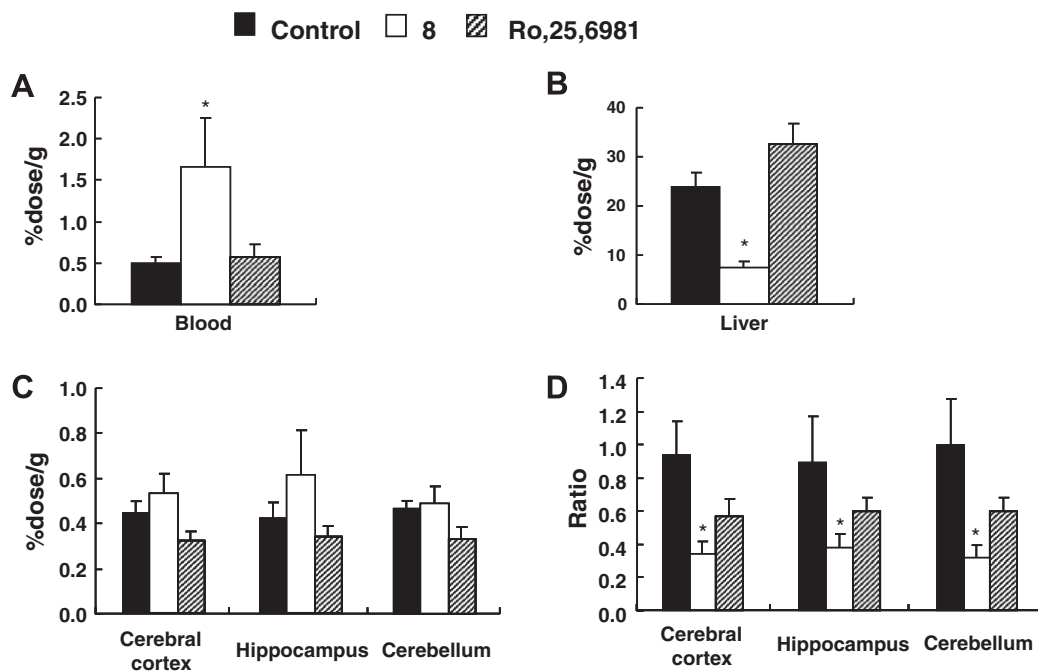
Figure 5. Effects of non-radioactive **8** and Ro-25,6981 (NR2B antagonist) on the blood concentration (A), liver uptake (B), regional brain uptake (C), and brain tissue to blood ratio (D) of [^{125}I]**8** in mice at 180 min after injection. Drugs (3 mg/kg) were given as pre-treatment by intravenous injection 30 min before [^{125}I]**8** (148 kBq) administration. Values were presented as mean ± SD (% dose/g, $n = 5$). * $P < 0.01$ in comparison to the control group (Kruskal–Wallis test, post-test was Dunn's test).

Table 4
The modulation of BBB permeability of [125I]**8** by P-glycoprotein[a]

	Control	Cyclosporin A (50 mg/kg)
Blood	0.78 ± 0.27	0.52 ± 0.26
Liver	16.20 ± 1.34	15.20 ± 5.71
Kidney	4.49 ± 1.34	4.80 ± 0.69
Brain	0.50 ± 0.04	0.66 ± 0.22
Brain/blood	0.74 ± 0.41	1.16 ± 0.36

[a] Regional organ uptake at 180 min after [125I]**8** injection. Cyclosporin A (50 mg/kg) was given as pre-treatment by intravenous injection 30 min before [125I]**8** (148 kBq) administration. Values were presented as mean ± SD (% dose/g, n = 5).

Table 5
The modulation of BBB permeability of [125I]**8** by organic anion transporter[a]

	Control	Probenecid (200 mg/kg)
Blood	0.46 ± 0.07	0.41 ± 0.11
Brain	0.44 ± 0.06	0.57 ± 0.19
Liver	19.13 ± 2.09	20.03 ± 5.81
Kidney	6.29 ± 1.47	4.20 ± 0.97
Brain/blood	0.98 ± 0.13	1.43 ± 0.37

Values were presented as mean ± SD (% dose/g, n = 5). *P <0.05 in comparison to the control group (Mann–Whitney U-test).
[a] Regional organ uptake at 180 min after [125I]**8** injection. Probenecid (200 mg/kg) was given as pre-treatment by intravenous injection 30 min before [125I]**8** (148 kBq) administration.

strated no reduction by treatment with probenecid (Table 5). It is reported that probenecid is the substrate of OAT1 and 3. OAT1 is mainly expressed in the kidney and OAT3 in the kidney and brain. OATs play a role in the renal influx of probenecid.[40,41] Therefore, this study indicated that [125I]**8** may be a substrate of OATs in the brain and kidney. Although the extent of transport via P-gp and OAT is thought to be minimal, a certain amount of [125I]**8** that enters the brain might serve as substrate of P-gp and OAT. Since it is reported that numerous structurally and pharmacologically unrelated lipophilic and amphipathic organic compounds are substrate of P-gp,[42] the structural relationship between benzimidazoles and P-gp substrate is not elucidated. The introduction of a non-acidic group instead of a hydroxyl group in the benzimidazole skeleton of [125I]**8** is expected to reduce the efflux by OAT. Furthermore, reduced lipophilic property of [125I]**8** should be necessary to increase BBB permeability.

Another problem is the homogeneous distribution of [125I]**8** and [125I]**9** observed in the brain tissues under in vivo condition, which was quite different from in vitro results. Various factors might be present under in vivo condition such as non-specific binding to capillary endothelial cells or other region. It is unclear whether the radioactivity of regional brain is present in the target site or peripheral site. However the benzimidazoles with optimized log P values might decrease an accumulation in peripheral region.

Similar to this study, previously reported imaging agents for NR2B subunit of NMDA receptor showed consistent accumulation pattern with the expression of NR2B subunit and high specificity to NR2B rich region only under in vitro condition but not in vivo.[13–19] Moreover, similar binding characters were observed in the radioligands for other binding sites of NMDA receptor, such as ion-channel site[43,44] and glycine site.[45–47] Kew et al. suggested that ifenprodil might exhibit higher affinity for the agonist-bound activated and desensitized states of the NMDA receptor, respectively, relative to the resting, agonist-unbound state.[48] Furthermore, Mott et al. demonstrated that NR2B antagonists were much more potent as a neuroprotectant at pH 6.5 than at pH 7.5.[49] The pH of ischemic tissue is as low as 6.5.[50] In like manner, it is reported that [125I]CNS-1261, a radioligand for ion-channel site of NMDA receptor, showed higher uptake in the ischemic rat brain

than normal region.[51] In lieu with these reports, it is conjectured that the different biodistribution patterns of radioligands for the NR2B subtype of the NMDA receptor could be observed between normal condition and overactivated state, such as pathological stage.

Since [125I]**8** and [125I]**9** showed low brain uptake and homogeneous brain distribution, these ligands were unsuitable for SPECT imaging of cerebral NMDA receptors. However, it should be noted that [125I]**8** may have specific binding component in the NR2B subunit in vivo. The present study indicated that benzimidazole derivatives may be potential lead compounds for developing novel imaging agents for the NR2B subtype of NMDA receptors. Further structure–activity relationship studies are required.

3. Conclusion

Our study has developed high-affinity benzimidazole derivatives **8** and **9** as new SPECT ligand candidates for NR2B subunit of the NMDA receptor. In vitro autoradiography experiments demonstrated that [125I]**8** and [125I]**9** showed NR2B selective binding in the rat brain slices. Although [125I] benzimidazoles showed poor BBB permeability and inconsistent distribution with NR2B subunit, [125I]**8** may be partially bound to the NR2B subunit under in vivo condition. Compound **8** may be a potential scaffold for further structural modification to develop novel imaging probes of cerebral NMDA receptors.

4. Experimental section

4.1. General information

¹H NMR spectra were recorded on a JNM-GSX-270WB spectrometer (270 MHz; JEOL, Tokyo, Japan), using tetramethylsilane as an internal standard. Fast atom bombardment mass spectra (FAB-MS) were obtained on a JMS-AX505H spectrometer (JEOL). Electrospray ionization mass spectra (ESI-MS) were obtained on a TSQ 7000 (Thermo Fisher Scientific, California, USA). High-resolution mass spectra (HRMS) were obtained on a QSTAR®XL MS/MS System with the use of ESI. [125I]NaI was purchased from MP Biomedicals (California, USA). All other chemicals used were reagent grade. All animals were supplied by Japan SLC (Hamamatsu, Japan). An automated gamma counter with a NaI(Tl) detector (ARC-2000; Aloka, Tokyo, Japan) was used to measure radioactivity. The present animal study was approved by the Animal Care and Use Committee of the Hamamatsu University School of Medicine.

4.1.1. Ethyl 2-{4-(4-bromobenzyl)piperidin-1-yl} acetate (4)

To a solution of **3**[23] (13.0 g, 51.15 mmol) in DMF (8.0 ml), diisopropylethylamine (10.65 ml, 61.26 mmol), and ethyl bromoacetate (6.84 ml, 61.26 mmol) were added, and the reaction mixture was stirred at room temperature for 3 h. EtOAc (50 ml) was added to the mixture, and the organic layers were washed with aqueous NaHCO₃ and brine, dried with Na₂SO₄, and evaporated to dryness. The crude product was chromatographed on silica gel with hexane/EtOAc = 2:1 to provide **4** (12.4 g, 36.44 mmol, 71%) as a colorless oil, ¹H NMR (CDCl₃) δ: 7.38 (2H, d, J = 8.43 Hz), 7.01 (2H, d, J = 8.42 Hz), 4.17 (2H, q, J = 7.33 Hz), 3.17 (2H, s), 2.90 (2H, d, J = 11.92 Hz), 2.48 (2H, d, J = 6.59 Hz), 2.10 (2H, t, J = 11.54 Hz), 1.58–1.33 (5H, m), 1.26 (3H, t, J = 7.15 Hz), ESI-MS m/z; 340 (M+H)⁺.

4.1.2. Ethyl 2-{4-(4-tributylstannylbenzyl)piperidin-1-yl} acetate (5)

To a solution of **4** (5.0 g, 14.69 mmol) in toluene (50 ml), bistributyltin (14.7 ml, 29.38 mmol), and tetrakis (triphenylphosphine) palladium (509 mg, 0.44 mmol) were added, and the reaction mix-

ture was refluxed for 36 h. After cooling, the reaction mixture was filtered through Celite. The filtrate was evaporated to dryness. The crude product was chromatographed on silica gel with hexane/EtOAc = 3:1 to provide **5** (4.30 g, 7.75 mmol, 53%) as a colorless oil, ^{1}H NMR (CDCl$_3$) δ: 7.35 (2H, d, J = 7.35 Hz), 7.09 (2H, d, J = 7.90 Hz), 4.17 (2H, q, J = 7.16 Hz), 3.17 (2H, s), 2.91 (2H, d, J = 11.54 Hz), 2.50 (2H, d, J = 6.61 Hz), 2.10 (2H, t, J = 11.43 Hz), 1.66–1.23 (20H, m), 1.06–0.85 (15H, m), FAB-MS m/z; 552 (M+H)$^+$.

4.1.3. Ethyl 2-{4-(4-iodobenzyl)piperidin-1-yl} acetate (6)

To a stirred solution of **5** (2.85 g, 5.17 mmol) in carbon tetrachloride (135 ml), 50 mM solution of iodine in dry carbon tetrachloride (135 ml, 6.72 mmol) was added dropwise, and the reaction mixture was allowed to stand at room temperature for 1 h. The mixture was evaporated to dryness. The crude product was chromatographed on silica gel with hexane/EtOAc = 1:1 to provide **6** (1.36 g, 3.51 mmol, 68%) as a colorless oil, ^{1}H NMR (CDCl$_3$) δ: 7.58 (2H, d, J = 8.33 Hz), 6.88 (2H, d, J = 8.33 Hz), 4.17 (2H, q, J = 7.08 Hz), 3.17 (2H, s), 2.90 (2H, d, J = 11.54 Hz), 2.47 (2H, d, J = 6.41 Hz), 2.10 (2H, t, J = 11.54 Hz), 1.62–1.34 (5H, m), 1.26 (3H, t, J = 7.16 Hz), FAB-MS m/z; 388 (M+H)$^+$.

4.1.4. 2-{[4-(4-Iodobenzyl)piperidin-1-yl]methyl}-5-methoxybenzimidazole (7)

Compound **6** (804 mg, 2.08 mmol) was dissolved in 6 M HCl (5 ml), and the mixture was heated to 100 °C for 1 h. The reaction mixture was cooled and evaporated to dryness. The residue was dissolved in DMF (6 ml), followed by EDC (518 mg, 2.70 mmol), 1-hydroxy-7-azabenzotriazole (367 mg, 2.70 mmol), triethylamine (570 µl, 4.16 mmol), and 4-methoxy-1,2-phenylenediamine (287 mg, 2.08 mmol). The reaction mixture was stirred at room temperature for 3 h followed by quenching with aqueous NaHCO$_3$ and ethyl acetate. Organic layer was separated and washed by brine, dried with Na$_2$SO$_4$, and evaporated to dryness. The crude oil was dissolved in acetic acid (6 ml) and heated to 140 °C for 4 h. The reaction mixture was cooled and evaporated to dryness. The crude product was chromatographed on silica gel with CHCl$_3$/MeOH = 20:1 to provide **7** (530 mg, 1.15 mmol, 55%) as a colorless oil, ^{1}H NMR (CDCl$_3$) δ: 7.59 (2H, d, J = 8.12 Hz), 7.46 (1H, d, J = 7.91 Hz), 7.04 (1H, s), 6.88 (1H, d, J = 8.12 Hz), 6.87 (1H, d, J = 7.98 Hz), 3.85 (5H, s), 2.93 (2H, d, J = 12.18 Hz), 2.51 (2H, d, J = 6.41 Hz), 2.21 (2H, t, J = 11.33 Hz), 1.68–1.25 (5H, m), ESI-MS m/z; 462 (M+H)$^+$.

4.1.5. 2-{[4-(4-Iodobenzyl)piperidin-1-yl]methyl}benzimidazol-5-ol (8)

Compound **7** (530 mg, 1.15 mmol) was dissolved in HBr/H$_2$O (48%, 10 ml), and the mixture was heated to 100 °C for 6 h. The reaction mixture was cooled and evaporated to dryness. The crude product was chromatographed on silica gel with CHCl$_3$/MeOH/NH$_4$OH = 200:10:1 to provide **8** (324 mg, 0.724 mmol, 63%) as a white solid, mp = 117–118 °C, ^{1}H NMR (CDCl$_3$) δ: 7.67 (1H, dd, J = 8.66, 1.01 Hz), 7.63 (2H, d, J = 8.55 Hz), 7.16–7.12 (2H, m), 6.99 (2H, d, J = 8.34 Hz), 4.77 (2H, s), 3.63 (2H, d, J = 11.97), 3.26–3.17 (1H, m), 2.58 (d, J = 6.84 Hz), 1.95–1.90 (4H, m), 1.66–1.60 (2H, m), ESI-HRMS (m/z) calcd for C$_{20}$H$_{23}$IN$_3$O, 448.0880 (M+H)$^+$, obsd 448.0829.

4.1.6. N-{2-[4-(4-Iodobenzyl)-piperidin-1-ylmethyl]benoimidazol-5-yl}-methanesulfonamide (9)

Using the above procedure for **7** with N-(3,4-diaminophenyl)methanesulfonamide,[20] the title compound **9** (27 mg, 0.052 mmol, 53%) was obtained as a white solid, mp = 92–94 °C, ^{1}H NMR (CD$_3$OD) δ: 7.58 (2H, d, J = 8.34 Hz), 7.50 (1H, d, J = 8.12 Hz), 7.49 (1H, dd, J = 2.08, 0.48 Hz), 7.13 (1H, dd, J = 8.66, 2.04 Hz), 6.93 (2H, d, J = 7.91 Hz), 3.75 (2H, s), 3.32 (2H, d, J = 10.47 Hz), 2.90 (3H,

s), 2.50 (2H, d, J = 6.62 Hz), 2.11 (2H, t, J = 10.69 Hz), 1.64–1.20 (5H, m), ESI-HRMS (m/z) calcd for C$_{21}$H$_{26}$IN$_4$O$_2$S, 525.0821 (M+H)$^+$, obsd 525.0769.

4.1.7. Ethyl 2-{4-(4-Iodophenoxy)piperidin-1-yl} acetate (11)

Compound **10** (686 mg, 1.70 mmol)[25] was dissolved in 30% TFA/CH$_2$Cl$_2$ (5 ml), and the mixture was stirred at room temperature for 5 h followed by evaporated to dryness. The crude product was converted to the title compound **11** using the above procedure for compound **4**. In result, compound **11** (300 mg, 45%) was obtained as a colorless oil, ^{1}H NMR (CDCl$_3$) δ: 7.53 (2H, d, J = 8.98 Hz), 6.68 (2H, d, J = 8.98 Hz), 4.30 (1H, quin, J = 3.85 Hz), 4.19 (2H, q, J = 7.09 Hz), 3.24 (2H, s), 2.83–2.75 (2H, m), 2.58–2.47 (2H, m), 2.05–1.97 (2H, m), 1.91–1.84 (2H, m), ESI-MS m/z; 390 (M+H)$^+$.

4.1.8. 2-{[4-(4-Iodophenoxy)piperidin-1-yl]methyl}-5-methoxybenzimidazole (12)

Using the above procedure for **7** starting from compound **11**, the title compound **12** (96 mg, 0.207 mmol, 73%) was obtained as a yellow solid, mp = 50–52 °C, ^{1}H NMR (CD$_3$OD) δ: 7.53 (2H, d, J = 8.97 Hz), 7.41 (1H, d, J = 8.76 Hz), 7.04 (1H, d, J = 2.13 Hz), 6.86 (1H, dd, J = 8.76, 2.57 Hz), 6.73 (2H, d, J = 8.98 Hz), 4.38 (1H, quin, J = 3.74 Hz), 3.83 (3H, s), 3.79 (2H, s), 2.85–2.77 (2H, m), 2.51–2.41 (2H, m), 2.07–1.98 (2H, m), 1.87–1.77 (2H, m), ESI-MS m/z; 164 (M+H)$^+$.

4.1.9. 2-{[4-(4-Iodophenoxy)piperidin-1-yl]methyl}benzimidazol-5-ol (13)

Using the above procedure for **8** starting from compound **12**, the title compound **13** (108 mg, 0.241 mmol, 77%) was obtained as a white solid, mp = 63–65 °C, ^{1}H NMR (CD$_3$OD) δ: 7.53 (2H, d, J = 8.98 Hz), 7.34 (1H, d, J = 8.55 Hz), 6.90 (1H, d, J = 2.25 Hz), 6.74 (1H, dd, J = 8.45, 2.68 Hz), 6.73 (2H, d, J = 8.97 Hz), 4.38 (1H, quin, J = 3.63 Hz), 3.76 (2H, s), 2.86–2.76 (2H, m), 2.49–2.41 (2H, m), 2.07–1.99 (2H, m), 1.86–1.77 (2H, m), ESI-HRMS (m/z) calcd for C$_{19}$H$_{21}$IN$_3$O$_2$, 450.679 (M+H)$^+$, obsd 450.0621.

4.1.10. 2-{[4-(4-Trimethylstannylbenzyl)piperidin-1-yl]methyl}benzimidazol-5-ol (14)

To a solution of **8** (50 mg, 0.125 mmol) in toluene (3 ml), bis-trimethyltin (104 µl, 0.502 mmol), and tetrakis (triphenylphosphine) palladium (15 mg, 0.013 mmol) were added, and the reaction mixture was refluxed for 6 h. After cooling, the reaction mixture was filtered through Celite. The filtrate was evaporated to dryness. The crude product was chromatographed on silica gel with CHCl$_3$/MeOH = 15:1 to provide **14** (32 mg, 0.066 mmol, 53%) as a colorless oil, ^{1}H NMR (CDCl$_3$) δ: 7.41 (1H, d, J = 8.80 Hz), 7.39 (2H, d, J = 8.06 Hz), 7.08 (2H, d, J = 7.69 Hz), 7.04 (1H, d, J = 2.20 Hz), 6.83 (1H, dd, J = 8.80, 2.20 Hz), 4.09 (2H, s), 3.11 (2H, d, J = 12.09 Hz), 2.53 (2H, d, J = 5.87 Hz), 2.47 (2H, t, J = 11.73 Hz), 1.77–1.51 (5H, m), 0.27 (9H, s), FAB-MS m/z; 486 (M+H)$^+$.

4.1.11. N-{2-[4-(4-Trimethylstannylbenzyl)-piperidin-1-ylmethyl]benzoimidazol-5-yl}-methanesulfonamide (15)

Using the above procedure for **14** starting from compound **9**, the title compound **15** (5.2 mg, 9.26 µmol, 97%) was obtained as a colorless oil, ^{1}H NMR (CDCl$_3$) δ: 7.57–7.53 (2H, m), 7.40 (2H, d, 7.91 Hz), 7.18 (1H, d, 8.33 Hz), 7.10 (2H, d, 7.70 Hz), 3.78 (2H, s), 2.97 (3H, s), 2.86 (2H, d, J = 11.12 Hz), 2.54 (2H, d, J = 6.62 Hz), 2.14 (2H, t, J = 10.15 Hz), 1.41–1.22 (5H, m), 0.27 (9H, s), FAB-MS m/z; 563 (M+H)$^+$.

4.2. Radiosynthesis

[^{125}I]**8** and [^{125}I]**9** were prepared by similar method described in the literature.[26] In brief, 30% aqueous hydrogen peroxide (100 µl)

was added to a mixture of [^{125}I] NaI (60 μl, 19.4–41.4 MBq, carrier-free), 1% HCl (40 μl), and trimethylstannyl precursor **14**, **15** (0.1 mg in 100 μl of ethanol) in a sealed vial. The mixture was allowed to react for 40 min at room temperature and then quenched with 10% aqueous sodium bisulfite (100 μl). EtOAc (5 ml) was added to the mixture, and the organic layers were washed with aqueous brine, and evaporated to dryness. The crude products were purified by HPLC (column; Nacalai Cosmosil 5C18-AR II, 10 × 250 mm, mobile phase; MeOH: 0.1% TFA in H$_2$O = 60:40, flow rate: 3.0 ml/min). Each fraction was collected and the solvent was removed in vacuo. Radiochemical purity was assayed to be >98% by analytical HPLC (column; Nacalai Cosmosil 5C18-ARII, 4.6 × 250 mm, mobile phase; MeOH: 0.1% TFA in H$_2$O = 55:45, flow rate: 1.0 ml/min). The radiochemical yields based on [^{125}I] NaI were 85–90% and 78-81% for [^{125}I]**8** and [^{125}I]**9**, respectively.

4.3. In vitro binding assays

The K_i values of benzimidazoles for binding of [^{3}H]ifenprodil to rat cortical membrane homogenates were determined by the method mentioned in the literature.[25] In brief, well washed membranes (200–300 μg of protein) in 20 mM HEPES-KOH buffer (pH 7.4), were incubated with [^{3}H]ifenprodil (4.0 nM) with either buffer or displacing drug added to make a final volume of 500 μl for 120 min at 25 °C. In each experiment the assay buffer contained 100 mM trifluoroperazine. Non-specific binding was defined by the addition of unlabeled ifenprodil at 1 mM. Bound ligands were collected by rapid filtration using a Brandel cell harvester onto glass fiber filter (GF/B). The filters were washed rapidly three times with 2.5 ml of ice-cold assay buffer. Following separation and rinsed, the filters were placed into scintillation liquid (4 ml; ASCII, GE Healthcare Bio-Sciences) and radioactivity was determined with a liquid scintillation counter.

4.4. In vitro receptor autoradiography

The brain sagittal sections, obtained by the method described in the literature,[13] were pre-incubated for 30 min at 25 °C in 50 mM Tris–HCl buffer (pH 7.4 at 25 °C) containing 5% bovine serum albumin (BSA). These were subsequently incubated in the same buffer containing [^{125}I]**8** or [^{125}I]**9** (300 kBq, 0.09–0.14 nM) at 25 °C for 30 min. The slices were rinsed triplicate for 3 min each with cold (5 °C) incubation buffer containing 1% BSA, and subsequently dipped into cold water. The sections were dried under a steam of warm air and placed in contact with ^{125}I-sensitive imaging plates (BAS-SR 2040; Fuji Photo. Film, Tokyo, Japan) for 3 days. Distributions of radioactivity on the plates were analyzed by Bio-Image Analyzer (FLA-3000; Fuji Photo. Film, Tokyo, Japan), which were photographically visualized as shown in Figure 3A–D. Regions of interest (ROIs) on the slices were placed on the cerebral cortex, hippocampus, and cerebellum; and the radioactivities in these regions were expressed as photostimulated luminescence (PSL) values on ROI-background PSL value per square millimeter. The specific binding was determined as the difference between total binding and binding in the presence of the corresponding non-radioactive benzimidazoles (10 μM). Receptor selectivity studies were performed as similar procedure in the presence of several drugs (10 μM).

4.5. In vivo experiments

The [^{125}I] benzimidazoles (0.1 ml, ca. 14.8 kBq for whole body distribution studies, ca. 148 kBq for regional brain distribution studies) were injected intravenously via tail vein into ddY mice (male, 6 W, 30–35 g). At the designated time intervals, the mice were killed and their organs were dissected. The brain was further divided into the cerebral cortex, hippocampus, and cerebellum. The tissues were then weighed and the radioactivity was measured by automated gamma counting. Data were calculated as the percentage of the injected dose per gram of tissue (% dose/g).

To assess the in vivo specific binding of [^{125}I]**8**, the non-radioactive **8** or NR2B antagonist Ro-25,6981 (3 mg/kg in 10% DMSO/saline) was given as pre-treatment by intravenous injection 30 min before [^{125}I]**8** administration. Mice were killed 180 min after injection. The modulation of [^{125}I]**8** by P-gp and OAT in vivo was evaluated according to the literature.[36,52,53] In brief, CsA {50 mg/kg in a mixture of cremophor EL (140 mg/ml) and ethanol (5%)/saline} or probenecid (200 mg/kg in 5% sodium bicarbonate/saline) was given as pre-treatment by intravenous injection 30 min before [^{125}I]**8** administration. Mice were killed 180 min after injection of [^{125}I]**8**. In each of the control mouse, the same amount of drug-free corresponding solvent was injected.

To assess the metabolism of [^{125}I] benzimidazoles in the mouse brain, the mice were killed at 180 min after [^{125}I] benzimidazoles (185 kBq) injection. Whole brains were quickly removed, homogenized with ice-cooled MeOH (1.0 ml), and centrifuged at 1750g for 10 min at 4 °C. The metabolites in MeOH extract were analyzed by radio-TLC using CHCl$_3$/MeOH = 9:1 and EtOAc/EtOH = 1:1 for [^{125}I]**8**, CHCl$_3$/EtOH = 4:1 and EtOAc/EtOH = 4:1 for [^{125}I]**9**, as mobile phases.

4.6. Partition co-efficient determination

Partition co-efficient between n-octanol and buffer was measured by a conventional shake flask method in triplicate. The benzimidazoles (1–2 mg) were well shaken in a mixture of n-octanol (1 ml) and 10 mM phosphate buffer (pH 7.4, 1 ml) for 15 min at ambient temperature. After centrifugation (2500 rpm for 5 min) of the mixture, the two layers were separated and analyzed by HPLC (column; Nacalai Cosmosil 5C$_{18}$-AR 300, 4.6 × 250 mm, mobile phase; MeOH: 0.1% TFA in H$_2$O = 50:50, flow rate: 1.0 ml/min) to obtain log D (pH 7.4) values (Table 1).

4.7. Data analysis

Data were expressed as the mean ± standard deviation. In vitro experiments of [^{125}I]**8** and [^{125}I]**9** were statistically analyzed by Mann–Whitney U-test as shown in Figure 2. In vivo experiments of [^{125}I] **8** were analyzed by the Kruskal–Wallis test with Dunn's multiple comparison post-test as shown in Figure 4 or Mann–Whitney U-test as shown in Table 4. A value of P <0.05 was considered statistically significant.

Acknowledgments

References and notes

1. Danysz, W.; Parsons, C. G. Pharmacol. Rev. **1998**, 50, 597.
2. Rothman, S. M.; Olney, J. W. Ann. Neurol. **1986**, 19, 105.
3. Meldrum, B.; Garthwaite, J. Trends Pharmacol. Sci. **1990**, 11, 379.
4. Francis, P. T.; Sims, N. R.; Procter, A. W.; Bowen, D. M. J. Neurochem. **1993**, 60, 1589.
5. Beal, M. F.; Swartz, K. J.; Isacson, O. Dev. Brain Res. **1992**, 68, 136.
6. Moore, H.; West, A. R.; Grace, A. A. Biol. Psychiatry **1999**, 46, 40.
7. Dingledine, R.; Borges, K.; Bowie, D.; Traynelis, S. F. Pharmacol. Rev. **1999**, 51, 7.
8. Masu, M.; Nakajima, Y.; Moriyoshi, K.; Ishii, T.; Akazawa, C.; Nakanashi, S. Ann. N.Y. Acad. Sci. **1993**, 707, 153.
9. Loftis, J. M.; Janowsky, A. Pharmacol. Ther. **2003**, 97, 55.

10. Liu, Y.; Wong, T. P.; Aarts, M.; Rooyakkers, A.; Liu, L.; Lai, T. W.; Wu, D. C.; Lu, J.; Tymianski, M.; Craig, A. M.; Wang, Y. T. *J. Neurosci.* **2007**, *27*, 2846.
11. DeRidder, M. N.; Simon, M. J.; Siman, R.; Auberson, Y. P.; Raghupathi, R.; Meaney, D. F. *Neurobiol. Dis.* **2006**, *22*, 165.
12. Zhou, M.; Baudry, M. *J. Neurosci.* **2006**, *26*, 2956.
13. Haradahira, T.; Maeda, J.; Okauchi, T.; Zhang, M. R.; Hojo, J.; Kida, T.; Arai, T.; Yamamoto, F.; Sasaki, S.; Maeda, M.; Suzuki, K.; Suhara, T. *Nucl. Med.Biol.* **2002**, *29*, 517.
14. Roger, G.; Lagnel, B.; Besret, L.; Bramoullé, Y.; Coulon, C.; Ottaviani, M.; Kassiou, M.; Bottlaender, M.; Valette, H.; Dollé, F. *Bioorg. Med. Chem.* **2003**, *11*, 5401.
15. Dollé, F.; Valette, H.; Demphel, S.; Coulon, C.; Ottaviani, M.; Bottlaender, M.; Kassiou, M. *J. Labelled Compd. Radiopharm.* **2004**, *47*, 911.
16. Roger, G.; Dollé, F.; Bruin, B.; Liu, X.; Besret, L.; Bramoullé, Y.; Coulon, C.; Ottaviani, M.; Bottlaender, M.; Valette, H.; Kassiou, M. *Bioorg. Med. Chem.* **2004**, *12*, 3229.
17. Haradahira, T.; Okauchi, J.; Maeda, J.; Suzuki, K.; Suhara, T. *J. Nucl. Med.* **2004**, *45*, 441P.
18. Haradahira, T.; Fuchigami, T.; Fujimoto, N.; Okauchi, T.; Maeda, J.; Suzuki, K.; Suhara, T.; Yamamoto, F.; Mukai, T.; Maeda, M. *J. Labelled Compd. Radiopharm.* **2005**, *48*, S92.
19. Arstad, E.; Platzer, S.; Berthele, A.; Pilowsky, L. S.; Luthra, S. K.; Wester, H. J.; Henriksen, G. *Bioorg. Med. Chem.* **2006**, *14*, 6307.
20. McCauley, J. A.; Theberge, C. R.; Romano, J. J.; Billings, S. B.; Anderson, K. D.; Claremon, D. A.; Freidinger, R. M.; Bednar, R. A.; Mosser, S. D.; Gaul, S. L. *J. Med. Chem.* **2004**, *47*, 2089.
21. Borza, I.; Kolok, S.; Gere, A.; Nagy, J.; Fodor, L.; Galgóczy, K.; Fetter, J.; Bertha, F.; Agai, B.; Horváth, C.; Farkas, S.; Domány, G. *Bioorg. Med. Chem. Lett.* **2006**, *16*, 4638.
22. Borza, I.; Bozó, E.; Barta-Szalai, G.; Kiss, C.; Tárkányi, G.; Demeter, A.; Gáti, T.; Háda, V.; Kolok, S.; Gere, A.; Fodor, L.; Nagy, J.; Galgóczy, K.; Magdó, I.; Agai, B.; Fetter, J.; Bertha, F.; Keserü, G. M.; Horváth, C.; Farkas, S.; Greiner, I.; Domány, G. *J. Med. Chem.* **2007**, *50*, 901.
23. Matsumoto, R.; Haradahira, T.; Ito, H.; Fujimura, Y.; Seki, C.; Ikoma, Y.; Maeda, J.; Arakawa, R.; Takano, A.; Takahashi, H.; Higuchi, M.; Suzuki, K.; Fukui, K.; Suhara, T. *Synapse* **2007**, *61*, 795.
24. Kikuchi, R.; Kusuhara, H.; Sugiyama, D.; Sugiyama, Y. *J. Pharmacol. Exp. Ther.* **2003**, *306*, 51.
25. Ting, P. C.; Lee, J. F.; Wu, J.; Umland, S. P.; Aslanian, R.; Cao, J.; Dong, Y.; Garlisi, C. G.; Gilbert, E. J.; Huang, Y.; Jakway, J.; Kelly, J.; Liu, Z.; McCombie, S.; Shah, H.; Tian, F.; Wan, Y.; Shih, N. Y. *Bioorg. Med. Chem. Lett.* **2005**, *15*, 1375.
26. Kimball, F. S.; Romero, F. A.; Ezzili, C.; Garfunkle, J.; Rayl, T. J.; Hochstatter, D. G.; Hwang, I.; Boger, D. L. *J. Med. Chem.* **2008**, *51*, 937.
27. Coughenour, L. L.; Barr, B. M. *J. Pharmacol. Exp. Ther.* **2001**, *296*, 150.
28. Hirata, M.; Mori, T.; Soga, S.; Umeda, T.; Ohmomo, Y. *Chem. Pharm. Bull.* **2006**, *54*, 470.
29. Menniti, F.; Chenard, B.; Collins, M.; Ducat, M.; Shalaby, I.; White, F. *Eur. J. Pharmacol.* **1997**, *331*, 117.
30. Mori, H.; Mishina, M. *Neuropharmacology* **1995**, *34*, 1219.
31. Chenard, B. L.; Shalaby, I. A.; Koe, B. K.; Ronau, R. T.; Butler, T. W.; Prochniak, M. A.; Schmidt, A. W.; Fox, C. B. *J. Med. Chem.* **1991**, *34*, 3085.
32. Karbon, E. W.; Patch, R. J.; Pontecorvo, M. J.; Ferkany, J. W. *Eur. J. Pharmacol.* **1990**, *176*, 247.
33. Slifstein, M.; Hwang, D. R.; Martinez, D.; Ekelund, J.; Huang, Y.; Hackett, E.; Abi-Dargham, A.; Larelle, M. *J. Nucl. Med.* **2006**, *47*, 313.
34. Frankle, W. G.; Slifstein, M.; Gunn, R. N.; Huang, Y.; Hwang, D. R.; Darr, E. A.; Narendran, R.; Abi-Dargham, A.; Laruelle, M. *J. Nucl. Med.* **2006**, *47*, 815.
35. Dischino, D. D.; Welch, M. J.; Kilbourn, M. R.; Raichle, M. E. *J. Nucl. Med.* **1983**, *24*, 1030.
36. Ishiwata, K.; Kawamura, K.; Yanai, K.; Hendrikse, N. H. *J. Nucl. Med.* **2007**, *48*, 81.
37. Laćan, G.; Plenevaux, A.; Rubins, D. J.; Way, B. M.; Defraiteur, C.; Lemaire, C.; Aerts, J.; Luxen, A.; Cherry, S. R.; Melega, W. P. *Eur. J. Nucl. Med. Mol. Imaging* **2008**, *35*, 2256.
38. Nojiri, Y.; Ishiwata, K.; Qinggeletu; Tobiishi, S.; Sasada, T.; Yamamoto, F.; Mukai, T.; Maeda, M. *Biol. Pharm. Bull.* **2008**, *31*, 1274.
39. Mizuno, N.; Niwa, T.; Yotsumoto, Y.; Sugiyama, Y. *Pharmacol. Rev.* **2003**, *55*, 425.
40. Zhou, F.; You, G. *Pharm. Res.* **2007**, *24*, 28.
41. Masereeuw, R.; Russel, F. G. *Pharmacol. Ther.* **2010**, *126*, 200.
42. Zhou, S.; Lim, L. Y.; Chowbay, B. *Drug Metab. Rev.* **2004**, *36*, 57.
43. Orita, K.; Sasaki, S.; Maeda, M.; Hashimoto, A.; Nishikawa, T.; Yugami, T.; Umezu, K. *Nucl. Med. Biol.* **1993**, *20*, 865.
44. Haradahira, T.; Sasaki, S.; Maeda, M.; Kobayashi, K.; Inoue, O.; Tomita, U.; Nishikawa, T.; Suzuki, K. *J. Labelled Compd. Radiopharm.* **1998**, *41*, 843.
45. Haradahira, T.; Zhang, M. R.; Maeda, J.; Okauchi, T.; Kawabe, K.; Kida, T.; Suzuki, K.; Suhara, T. *Nucl. Med. Biol.* **2000**, *27*, 357.
46. Fuchigami, T.; Haradahira, T.; Fujimoto, N.; Okauchi, T.; Maeda, J.; Suzuki, K.; Suhara, T.; Yamamoto, F.; Sasaki, S.; Mukai, T.; Yamaguchi, H.; Ogawa, M.; Magata, Y.; Maeda, M. *Nucl. Med. Biol.* **2008**, *35*, 203.
47. Fuchigami, T.; Haradahira, T.; Fujimoto, N.; Nojiri, Y.; Mukai, T.; Yamamoto, F.; Okauchi, T.; Maeda, J.; Suzuki, K.; Suhara, T.; Yamaguchi, H.; Ogawa, M.; Magata, Y.; Maeda, M. *Bioorg. Med. Chem.* **2009**, *17*, 5665.
48. Kew, J. N.; Trube, G.; Kemp, J. A. *J. Physiol.* **1996**, *497*, 761.
49. Mott, D. D.; Doherty, J. J.; Zhang, S.; Washburn, M. S.; Fendley, M. J.; Lyuboslavsky, P.; Traynelis, S. F.; Dingledine, R. *Nat. Neurosci.* **1998**, *1*, 659.
50. Silver, I. A.; Erecinska, M. *J. Cereb. Blood Flow Metab.* **1992**, *12*, 759.
51. Owens, J.; Tebbutt, A. A.; McGregor, A. L.; Kodama, K.; Magar, S. S.; Perlman, M. E.; Robins, D. J.; Durant, G. J.; McCulloch, J. *Nucl. Med. Biol.* **2000**, *27*, 557.
52. Hesselink, M. B.; Smolders, H.; Eilbacher, B.; De Boer, A. G.; Breimer, D. D.; Danysz, W. *J. Pharmacol. Exp. Ther.* **1999**, *290*, 543.
53. Giri, N.; Shaik, N.; Pan, G.; Terasaki, T.; Mukai, C.; Kitagaki, S.; Miyakoshi, N.; Elmquist, W. F. *Drug Metab. Dispos.* **2008**, *36*, 1476.